Lymphology 57 (2024) 59-70

STAGING SYSTEM OF THREE-DIMENSIONAL NON-CONTRAST MAGNETIC RESONANCE LYMPHOGRAPHY IN SECONDARY LOWER EXTREMITY LYMPHEDEMA

T. Kageyama, Y. Shiko, Y. Kawasaki, T. Miyazaki, H. Sakai, R. Tsukuura, T. Yamamoto

Department of Plastic and Reconstructive Surgery, National Center for Global Health and Medicine, Tokyo, Japan (TK,TM,HS,RT,TY); Research Administration Center, Saitama Medical University, Tokyo, Japan (YS,YK)

ABSTRACT

Non-contrast magnetic resonance lymphography (NMRL) has been reported to be efficient for the evaluation of lymphedema. However, its characteristic findings and grading system are yet fully clarified. We retrospectively examined 48 patients with secondary lower extremity lymphedema (LEL) who underwent NMRL and indocyanine green lymphography (ICG-L). The lower extremity was divided into 5 areas for NMRL evaluation, and the prevalence of characteristic NMRL findings (Mist, Spray, and Inky) and the 3D NMRL stage that we proposed were compared according to the ICG-L stage. All characteristic NMRL findings increased in prevalence with the progression of the ICG-L stage (Mist, Spray, and Inky: $P < 0.001$, < 0.001, and < 0.001, respectively) Predominant findings in each segment changed significantly from Mist in the ICG-L stage 0-II, to the Spray in ICG-L stage III-IV, to the Inky in ICG-L stage V ($P < 0.001$). 3D NMRL stage significantly advanced with the progression of the ICG-L stage ($r_s = 0.72$; $P < 0.001$). We believe this severity grading system is useful for efficient evaluation of fluid accumulation in LEL patients.

Keywords: lymphedema, magnetic resonance lymphography, indocyanine green lymphography

Lower extremity lymphedema (LEL) is a chronic and progressive condition that occurs as a result of congenital or acquired impairments in the lymphatic circulation (1). Conservative treatment, including compression garments, elastic bandages, skin care, and manual lymph drainage, is the mainstay of LEL treatment (2,3). Recently, there has been an increasing trend in lymphaticovenular anastomosis (LVA) and vascularized lymph node transfer (VLNT) for lymphatic reconstruction (4). As a preoperative imaging modality for these surgeries, indocyanine green lymphography (ICG-L) has been widely recognized for its ability to visualize dermal backflow patterns in early stage of lymphedema, with several studies highlighting its effectiveness (5,6). However, unlike image modality for lymphatic circulation, there is currently no consensus on the optimal imaging method for the evaluation of fluid accumulation in lymphedematous limbs.

Several imaging modalities such as magnetic resonance lymphography, bioimpedance spectroscopy, ultrasonography, and computed tomography have been reported as excellent tools for investigating the detection of fluid

accumulation in lymphedematous limbs (7). Although bioimpedance has been recognized as highly valuable in evaluating fluid infiltration, its practical implementation in routine outpatient care can be challenging for many healthcare facilities (8,9). Ultrasonography has shown promise in assessing fluid infiltration, but its images can be influenced and limited by factors such as probe angles, ultrasonography frequency, and the expertise of the operator (10). Although computed tomography could also detect fluid accumulation, its contrast of water-rich structures is relatively weak as preoperative image inspections, and its sensitivity and specificity were still not fully investigated (11,12). In recent decades, several retrospective studies have highlighted the utility of non-contrast magnetic resonance lymphography (NMRL) for accurate and objective evaluation of fluid infiltration (13,14). Unlike contrast agent-based imaging techniques, NMRL can be employed for a wide range of patients, including those with asthma and renal dysfunction, without the risk of allergies.

Several characteristic MRL findings and grading systems of LEL in the coronal or horizontal sequence were reported by retrospective studies (15-17). However, the distinct findings and staging system of 3D sequences have not yet been clarified. As indocyanine green lymphography (ICG-L) has been widely used as an effective preoperative imaging modality, we employed ICG-L as an indicator of lymphatic circulation impairment to evaluate the characteristic NMRL findings associated with lymphedema (18). The purpose of this study is to assess the severity of 3D NMRL findings by comparing them with the ICG-L stage and to clarify the relationship between the 3D NMRL staging system and relevant parameters including the ICG-L stage and clinical parameters.

MATERIALS AND METHODS

This retrospective observational study was conducted at a single center and carried out under the approved protocol of the institutional review board (IRB) with the assigned approval number NCGM-S-004458-00. Written informed consent was waived as the study utilized only anonymous data. We analyzed data from 48 patients diagnosed with secondary LEL patients who had undertaken both NMRL and ICG-L between July 2017 and November 2021. Patients with other edematous diseases or a history of lower extremity surgery were excluded. A comprehensive set of examinations, including physical examination, blood and urine tests, chest X-ray, ultrasonography, and contrast-enhanced computed tomography, were conducted to rule out other edematous diseases such as heart failure, nephrosis, liver cirrhosis, and endocrine diseases. Patient characteristics, clinical findings, ICG-L findings, and NMRL findings were collected through a review of the patient's medical records.

Analysis of Clinical Data

The collected data included clinical parameters such as age, sex, body mass index (BMI), etiology of lymphedema, treatments for cancer, history of cellulitis, treatments for lymphedema, LEL index, the lymphedema quality of life assessment (LeQOLiS), ICG-L findings, NMRL findings, and the International Society of Lymphology (ISL) stage. The LeQOLiS questionnaire comprised of 10 items that assessed subjective lymphedematous symptoms (19). The scores obtained from these questions were summed up, ranging from 0 (the least severe symptoms) to 100 (the most severe symptoms), providing a quantitative measure of subjective symptoms associated with lymphedema. The LEL index was used as an indicator of lymphedematous swelling, as it allowed for a more accurate evaluation of limb volume considering individual body types, as compared to traditional volumetry methods (20).

NMRL Protocol

A 1.5-T Scanner (MAGNETOM Avanto, Siemens AG, Erlangen, Germany) was employed to acquire 3D SPACE T2 weighted image (T2WI) sequences. Patients were positioned supine with their feet first, and three

Table 1
Staging based on dermal backflow using ICG lymphography.

Dermal Backflow stage	ICG lymphography findings
Stage 0	Linear pattern only*
Stage I	Linear pattern + Splash pattern
Stage II	Linear pattern + Stardust pattern (1 region) **
Stage III	Linear pattern + Stardust pattern (2 regions) **
Stage IV	Linear pattern + Stardust pattern (3 regions) **
Stage V	Stardust pattern and/or Diffuse pattern***

* Dermal backflow pattern is not seen. ** Divided into 3 regions; the foot, lower leg, and thigh. *** Linear pattern is not seen. (Abbreviations: ICG = indocyanine green).

successive acquisitions were performed on the foot (first station), lower leg (second station), and thigh and pelvic areas (third station) using six-element phased-array coils. The matrix was 290x320 (phase resolution x base resolution) with a field of view of 480 x 480. Each acquisition consisted of thirty slices with a 2 mm section thickness. The scan time ranged from 3 to 5 minutes depending on the number of native slices. Evaluation of fluid distribution was conducted using 3D-SPACE images with a TR/TE of 2050/403 ms (effective TE: 115 ms).

ICG Lymphography Protocol

The ICG-L protocol involved the subcutaneous injection of 0.2 mL of ICG (Diagnogreen 2.5mg/mL; Daiichi Pharmaceutical, Tokyo, Japan) at the first web space of the foot and the lateral and medial border of the Achilles tendon. A 5% glucose water solution was used as solvent to minimize injection pain. Fluorescent images were captured immediately after injection and at 4 hours using an infrared camera system (PDE; Hamamatsu Photonics). We determined the ICG-L stage based on the dermal backflow stage classification, as summarized in *Table 1* (21).

Evaluation of Characteristic 3D NRML Findings

The evaluation of characteristic 3D NMRL findings involved assessing fluid accumulation, focusing on three distinct patterns: Mist, Spray, and Inky (*Fig. 1*). The definition of each pattern is listed in *Table 2*. The lower limb was divided into three segments for image analysis: the foot, lower leg, and thigh segments. Subsequently, the lower leg and thigh were further subdivided into medial and lateral areas, resulting in a total of five areas for

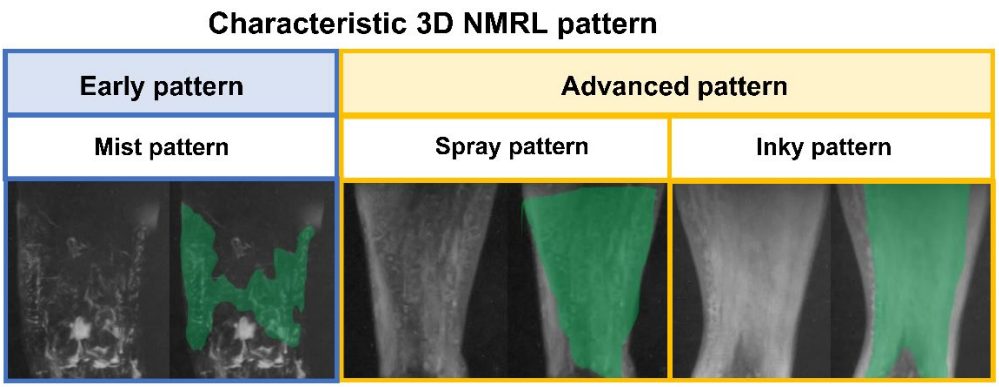

Fig. 1. *Characteristic findings of 3D NMRL include the early Mist pattern (left) and the advanced Spray (middle) and Inky (right) patterns.*

TABLE 2
Definitions of Characteristic 3D NMRL Findings for Mist, Spray, and Inky Patterns

NMRL Findings	Definition
Mist	Scattered high intensity dots against a low-intensity background (similar to Mist in the air).
Spray	Thick high intensity areas of dense concentration distributed extensively throughout the subcutaneous adipose layer.
Inky	Wider stripe-shaped high intensity area with clear boundaries in the extensive layer of subcutaneous fat (appears to be stripes painted with a paintbrush).

(Abbreviations: 3D = three-dimensional; NMRL = non-contrast magnetic resonance lymphography).

evaluating edema. The boundary between the thigh and lower leg was defined as the superior edge of the eminent intercondylar, while the boundary between the lower leg and foot was defined as the distal edge of the medial malleolus. Each pattern was considered present if its longitudinal length was more than one-fourth of the corresponding area in the lower extremities. In cases where multiple instances of the same type of edema were observed, the edema with the longest longitudinal length was adopted. In addition, we investigated the predominant pattern on the 3D NMRL sequence according to the ICG-L stage. The pattern with the longest length along the axis of the lower extremity was selected in each segment.

Severity Grading of 3D NMRL Stage

We proposed the 3D NMRL stage based on characteristic NMRL findings (*Table 3*). Limbs were divided into three segments of the thigh, lower leg, and foot. The definitions of severity stages were summarized and presented in *Fig. 2*. Based on our daily clinical experience, Mist pattern was considered an Early finding while Spray and Inky patterns were considered Advanced findings for a grading system. The foot was evaluated separately without considering the specific patterns of NMRL findings because distinguishing three NMRL patterns in the foot was difficult due to its small interstitial space and mixed high-intensity signals of blood vessels and joint effusion. The total numbers of the thigh and lower leg stages and the foot stages were defined as the 3D NMRL stage. Then, the 3D NMRL stage was compared with the ICG-L stage, BMI, LEL index, the ISL stage, scores of LeQOLiS, and duration of lymphedema.

TABLE 3
The 3D NMRL Stage Is Determined as the Sum of the Lower Leg, Thigh, and Foot Patterns

Stage	Stage of Lower leg and thigh	Stage of Foot
Stage 0	No fluid accumulation*	No fluid accumulation*
Stage Ⅰ	Early or Advanced patterns in one segment**	Early or Advanced patterns**
Stage Ⅱ	Early patterns in two segments**	
Stage Ⅲ†	Advanced patterns in one segment and Early patterns in two segments**	
Stage Ⅳ	Advanced patterns in two segments**	

* Fluid infiltration was not observed. ** The lower extremities were divided into 3 segments — the foot, lower leg, and thigh. Early patterns were Mist, while Advanced patterns were Spray and Inky. †From 3D NMRL stage Ⅲ, the existence of Advanced patterns is considered positive if the length of the pattern is more than 1/4 of each area. (Abbreviations: 3D = three-dimensional; NMRL = non-contrast magnetic resonance lymphography).

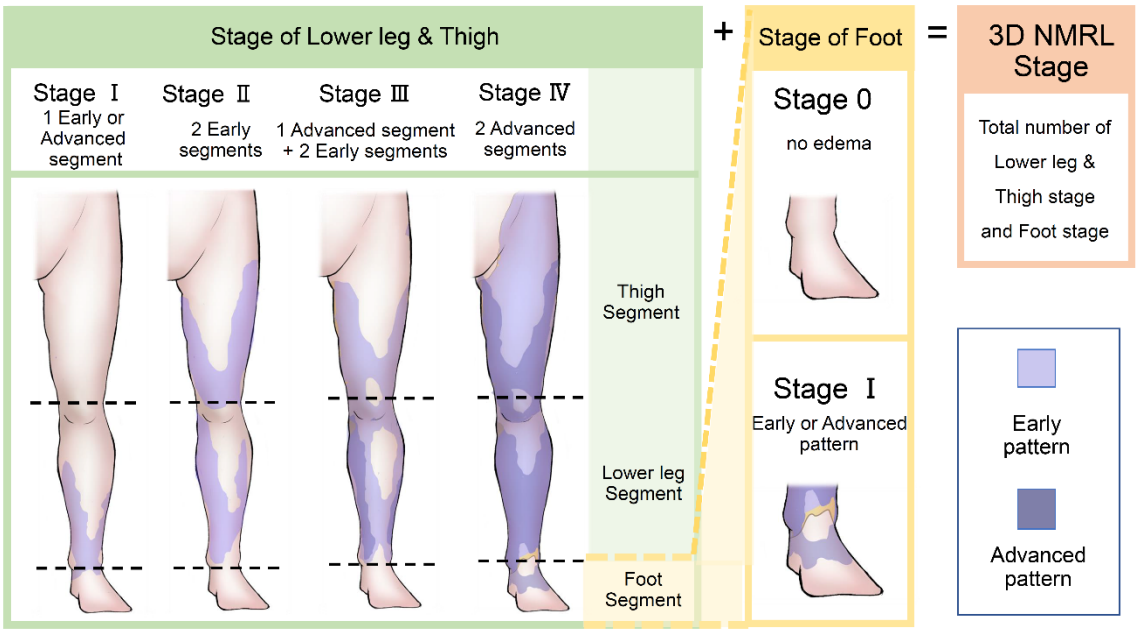

Fig. 2. *Schematic diagrams of the 3D NMRL image patterns based on characteristic 3D NMRL findings. The 3D NMRL stage of thigh and lower leg was determined based on the number of segments with Advanced patterns and Early patterns. The 3D NMRL stage was determined using the total numbers of the thigh and lower leg stages and the foot stages.*

Interobserver Agreement of 3D NMRL Stage

NMRL images were reviewed by two investigators consisting of a 4th-year plastic surgeon and a 2nd-year orthopedic surgeon. Two readers performed image evaluation independently with each reader blinded to all the clinical history and data. Weighted kappa with 95 percent CI and percentage agreement were used to assess the interobserver agreement on severity grading of the 3D NMRL stage among two readers. Any disagreement was resolved by the third reviewer who is a 4th-year plastic surgeon.

Statistical Analysis

The Cochran-Armitage trend test was employed to assess the prevalence of characteristic NMRL findings with the progression of the ICG-L stage. Fisher's exact test was employed to investigate the relationship between the representative NMRL findings and the ICG-L stage. Spearman's rank correlation coefficient (r_s) was utilized to examine the associations between the 3D NMRL stage, ICG-L stage, BMI, LEL index, ISL stage, LeQOLiS, and duration of lymphedema. Plus-minus values represented averages ± standard deviations. $P < 0.05$ was set as statistical significance. All statistical analysis was performed using JMP software (JMP 17 for Mac, SAS Institute, Cary, North Caronia).

RESULTS

A total of 48 patients were included. 43/48 patients (89.6%) were female, and 5/48 patients (10.4%) were male. Patients' characteristics are summarized in *Table 4*.

Characteristic 3D NMRL Findings in Each Segment of Lower Extremities

Mist, Spray, and Inky patterns had a significant difference in their prevalence between

TABLE 4
Patient Demographics

	Value
Age, yr	61.0 (range 35-84)
Sex (male: female)	5:43 (10.4%: 89.6%)
Body mass index, kg/m^2	23.23 (range 17.60-35.50)
History of radiation treatment	20/48 (41.7%)
History of chemotherapy	24/48 (50%)
History of cellulitis (n)	18/48 (37.5%)
Duration of lymphedema, mo	87.6 (range 1-480)
Compression therapy	27/48 (56.3%)
LEL index	259.5 (range 164-424)
Cause of Lymphedema	
Uterine cervical cancer	23/48 (47.9%)
Uterine corpus cancer	17/48 (35.4%)
Ovarian cancer	3/48 (6.3%)
Prostate cancer	2/48 (4.2%)
Other cancers	3/48 (6.3%)
ICG-L stage (n: limbs)	
0	20/96 (20.8%)
I	16/96 (16.7%)
II	20/96 (20.8%)
III	12/96 (12.5%)
IV	21/96 (21.9%)
V	7/96 (7.3%)
ISL stage (n)	
0	0/0 (0%)
I	19/48 (39.6%)
II	14/48 (29.2%)
III	15/48 (31.3%)

(Abbreviations: LEL = lower extremity lymphedema; ICG-L = indocyanine green lymphography; ISL = International Society of Lymphology).

the thigh, lower leg, and foot segments (P < 0.001, < 0.001, and < 0.001, respectively). There was a significant difference between the prevalence of Mist, Spray, and Inky patterns in all of the 480 areas (P < 0.001) (*Fig. 3A*). Mist pattern had the highest prevalence and the second highest was Spray pattern and Inky pattern had the lowest prevalence.

Characteristic 3D NMRL Patterns vs. ICG-L Stage

The prevalence of Mist, Spray, and Inky patterns increased with the progression of the ICG-L stage (P < 0.001, < 0.001, and < 0.001, respectively) (*Fig. 3 B-D*). In our study cohort, fluid accumulation on NMRL was observed in 94 of 96 limbs (97.9%) whereas dermal backflow on ICG-L was observed in 80 of 96 limbs (83.3%).

Prevalence of the predominant NMRL pattern showed a statistically significant difference according to the ICG-L stage (P < 0.001) (*Fig. 3E*). The most prevalent representative pattern significantly shifted from Mist pattern in ICG-L stage 0-II, to Spray pattern in the ICG-L stage III-IV, to Inky pattern in ICG-L stage V.

3D NMRL Stage vs. ICG-L Stage

There was a significant positive correlation between the 3D NMRL stage and the ICG-L stage (r_s = 0.72; P < 0.001) (*Fig. 3F*). The most prevalent 3D NMRL stage was stage I (7/20 patients, 35.0%) and stage II (7/20 patients, 35.0%) with the same high prevalence in ICG-L stage 0, stage II (7/16 patients, 43.8%) in ICG-L stage I, stage III (5/20 patients, 25.0%) in ICG-L stage II, stage IV (7/12 patients, 58.3%) in ICG-L stage III, stage V (17/21 patients, 81.0%) in ICG-L stage IV, and stage V (6/7 patients, 85.7%) in ICG-L stage V.

3D NMRL Stage vs. Clinical Demographics

The 3D NMRL stage didn't have a significant association with BMI and the ISL stage. However, LEL index, total scores, and scores of the distension, heaviness, pain, appearance, motor function, and social life on LeQOLiS became higher with progression of the 3D NMRL stage. The duration of lymphedema also was significantly longer as the 3D NMRL

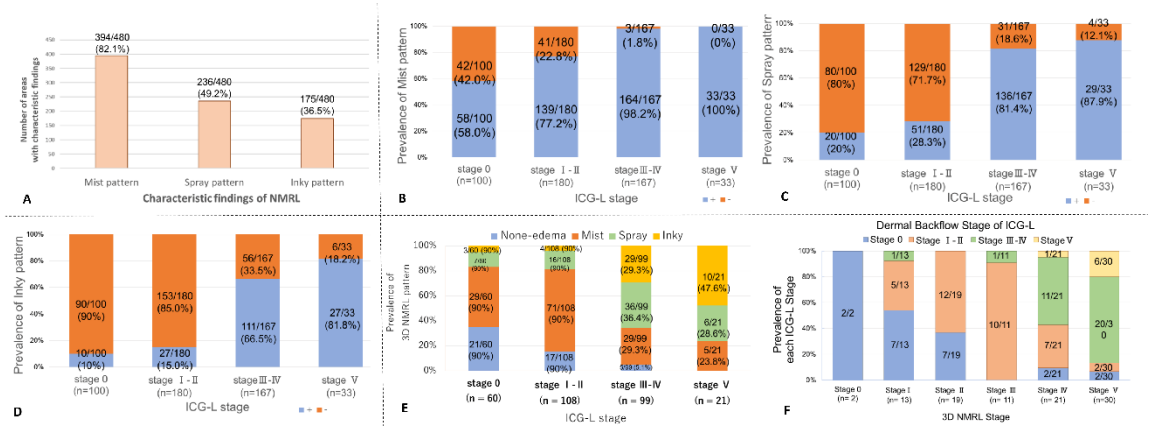

Fig. 3. *The prevalence of fluid infiltration on NMRL. The total prevalence of each pattern in all areas (P < 0.001) (A). The prevalence of Mist (B), Spray (C), and Inky (D) patterns according to the ICG-L stage (P < 0.001). The association between the prevalence of predominant NMRL findings and the ICG-L stage (P < 0.001) (E) and between the prevalence of the NMRL stage and the ICG-L stage (P < 0.001) (F).*

TABLE 5
Summary of the Statistical Analysis Compared the Severity Types of Fluid Distribution on NMRL with Clinical Parameters

	r_s	*p*
LEL	0.22	0.033*
index	0.18	0.078
BMI ISL	0.057	0.58
LeQOLiS		
Total scores of LeQOLiS	0.37	< 0.001**
Distention	0.40	< 0.001**
Heaviness	0.34	< 0.001**
Pain	0.21	0.041*
Dysesthesia	0.16	0.12
Appearance distortion	0.41	< 0.001**
Motor dysfunction	0.24	<0.019*
Limitation in daily activity	0.18	0.0721
Influence on social activity	0.34	< 0.001**
Distress caused by compression therapy	0.16	0.1092
Overall dissatisfaction caused by lymphedema	0.18	0.081
Duration of lymphedema	0.43	< 0.001**

* p value < 0.05; ** p value < 0.001. (Abbreviations: r_s = Spearman rank correlation coefficient; UEL index = Upper extremity lymphedema index; BMI = body mass index; ISL = International Society of Lymphology).

stage progressed. Statistical analysis comparing 3D NMRL stage and clinical parameters is summarized in *Table 5*.

Interobserver Agreement

Agreement for the severity grading of the 3D NMRL stage was 96.9 % (Weighted κ = 0.981; 95% CI, 0.96 to 1.00). The interobserver agreement for this grading system and characteristic 3D NMRL findings was almost perfect.

DISCUSSION

In this study, we demonstrated a statistically significant correlation between fluid accumulation on NMRL and impairment of lymphatic circulation on ICG-L. The 3D NMRL stage we proposed progressed with the advancement of the ICG-L stage and had positive significant correlations with the LEL index, LeQOLiS, and duration of lymphedema. Our results also showed that the predominant NMRL pattern in each segment significantly shifted from the Mist pattern in ICG-L stage 0-II, to the Spray pattern in ICG-L stage III-IV, and finally to the Inky pattern in ICG-L stage V, while the prevalence of each pattern in all areas decreased in the order of Mist, Spray, and Inky patterns. These results suggest that the Mist pattern is considered mild, the Spray pattern moderate, and the Inky pattern severe. The prevalence of all characteristic NMRL patterns increased with the progression of the ICG-L stage and the frequency of fluid infiltration in NMRL was higher than the frequency of dermal backflow on ICG-L. We believe that information regarding the severity grading of fluid distribution on 3D NMRL based on the pathophysiologic lymph circulation is valuable for lymphatic physicians.

The pioneering study by Gregl in 1985 first reported characteristic MRL findings related to LEL (22). Subsequent several studies reported distinct NMRL findings in coronal sequences such as Reticular and Honeycomb (23-25). In addition, the grading system of NMRL proposed by previous studies had a significant association with lymphatic circulation on ICG-L (13,14). However, these studies did not statistically investigate the severity of several characteristic NMRL findings in the 3D sequence and in addition, overlooked the edema on the foot area, despite its significant symptomatic relevance. This study's strength lies in elucidating the differences in severity among three characteristic 3D NMRL findings based on the ICG-L stage and proposing a practical 3D NMRL staging system for daily clinical use. The staging system distinguishes Early patterns (Mist) from Advanced patterns (Spray and Inky) thereby offering valuable insights for the management of lymphedema.

Our findings revealed a distinctive transition in predominant NMRL patterns from Mist to Spray to Inky which corresponded to the severity of the ICG-L stages (*Fig. 4*). The observed mechanism may be speculated as follows: in patients with mild ICG-L stages, valves between the lymphatic collector and precollector are reported to be damaged, leading to reverse flow from the collector to the precollector (26). This lymph flow dysfunction leads to small fluid accumulation in the interstitial space around fat lobules, and superficial and deep fascia, resulting in Mist pattern (*Fig. 4B*) (26). In moderate ICG-L stages, fluid accumulation extends and connects each other across superficial and deep fat layers, creating the Spray pattern (*Fig. 4C*). Severe ICG-L stages exhibit high-density fluid accumulation without non-edematous areas, manifesting as Inky pattern (*Fig. 4D*). Mist pattern generally covers the affected area with scattered regions lacking densely located fluid accumulation. In con-trast, Inky pattern exhibits comprehensive edema coverage with diffuse, high-intensity fluid accumulation throughout the area. This severity classification of NMRL findings based on anatomical structures can be highly valuable in the interpretation of 3D NMRL images.

Our results demonstrated that there was a strong correlation between the 3D NMRL stage and the ICG-L stage. Similar results were reported by retrospective MRL studies about LEL and upper extremity lymphedema (16,27-30). This phenomenon was expected presumably because the higher ICG-L stage

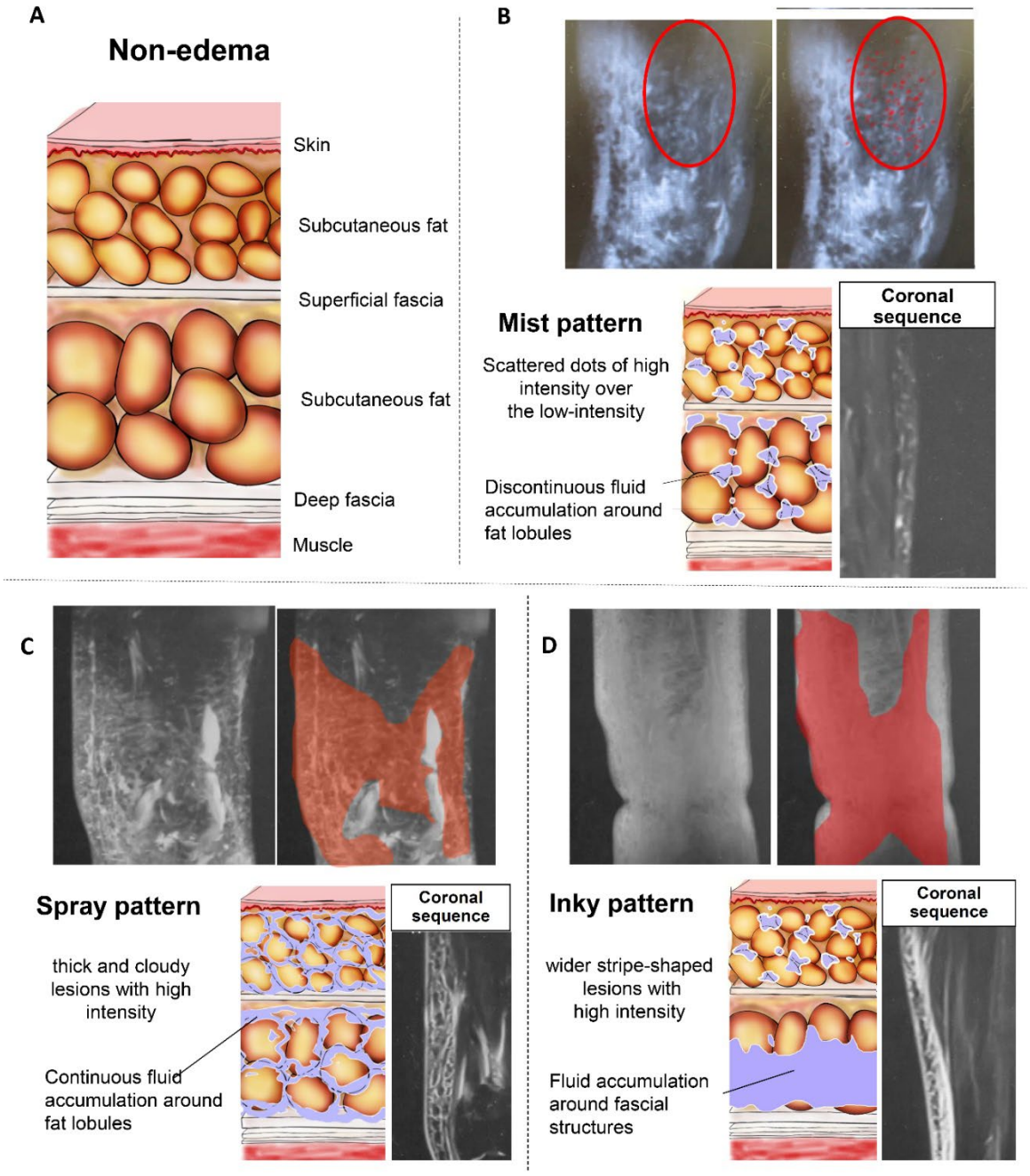

Fig. 4. *Diagrammatic and imaging correlation for characteristic NMRL Mist, Spray, and Inky patterns based on the anatomical structures of fat lobules, superficial and deep fascia, and dermis (A). Mist pattern included various small high intensity shapes scattered over a low-intensity background (B). Spray pattern consists of thick and cloudy lesions with high intensity, although it still contains some low-intensity areas (C). The Inky pattern presents as a wide stripe-shaped region with diffuse high intensity and almost no low-intensity areas (D).*

correlated with the inability to transfer lymph fluid in the proximal direction against gravity (31). This grading system also had a significant association with the total scores of LeQOLis and the duration of lymphedema. In contrast, the LEL index did not have a significant association with the ICG-L stage. The lack of significance in the LEL index may be due to the influence of measurement variability among different assessors on circumferential measurements. The 3D NMRL stage with almost perfect interobserver agreement may potentially allow for a visual and efficient assessment of edema localization through three-dimensional imaging.

Although various diagnostic tools and imaging modalities are used in the evaluation of fluid accumulation in lymphedematous limbs, NMRL can provide precise soft tissue contrast, especially for water, through non-invasive imaging (7). Its high-resolution images offer distinct anatomical information and can identify small fluid infiltration areas without contrast materials by suppressing fat. By comparing mild and severe NMRL findings, we can assess which areas should be prioritized for focused treatment. Furthermore, evaluating the efficacy of treatment interventions such as LVA and manual lymphatic drainage can be accomplished by comparing pre- and post-operative NMRL images of the treated areas. Moreover, the application of 3D NMRL staging has the potential to be valuable in determining the overall therapeutic effects on the lower limbs and prognostic predictions of each treatment by observing the temporal progression over time. Further research in this field is warranted to explore these aspects more comprehensively.

Limitations of this study include that the study was a monocentric retrospective observational study not externally validated by other centers' experiences. Another limitation is that this study only focused on fluid distribution and did not evaluate fat accumulation. As a result, it was technically difficult to investigate fat accumulation just due to lymphedema not other factors including obesity and lipedema. Lastly, this study focused on the use of the 3D-SPACE sequence and some institutions may not possess this sequence although several studies showed the 3D NMRL images in their reports. Further research with a large number of LEL patients is required to verify our results.

CONCLUSIONS

Three characteristic NMRL findings on 3D sequence revealed a significantly increasing severity from Mist to Spray and further to Inky. The 3D NMRL staging, which reflects the severity of these NMRL findings, showed significant correlations with the ICG-L stage and other clinical parameters including the circumferential limb swelling, and QOL scores. We believe that a detailed assessment of fluid accumulation in the lymphedematous limbs using 3D NMRL images is highly valuable for evaluating the effectiveness of lymphatic reconstruction procedures and various therapies.

CONFLICT OF INTEREST AND DISCLOSURE

The authors declare no competing financial interests exist.

REFERENCES

1. Lin, YS, CJ Liu: Predictors of severity of lymphosclerosis in extremity lymphedema. J. Vasc. Surg.-Venous L. 9 (2021), 00505-00509.
2. Warren, AG, H Brorson, LJ Borud, et al: Lymphedema: A comprehensive review. Ann. Plast. Surg. 59 (2007), 464–472.
3. Yamamoto, T, N Yamamoto, T Kageyama, et al: Technical pearls in lymphatic supermicrosurgery. Glob. Health Med. 29 (2020), 29-32.
4. Mark, VS, JC Christopher: Surgical treatment of lymphedema. Plast. Reconstr. Surg. 144 (2019), 738-758.
5. Yamamoto, T, N Yamamoto, K Doi, et al: Indocyanine green–enhanced lymphography for upper extremity lymphedema: A novel severity staging system using dermal backflow patterns. Plast. Reconstr. Surg. 128 (2011), 941.
6. Yamamoto, T, N Yamamoto: Indocyanine green lymphography for evaluation of breast lymphedema secondary to breast cancer

treatments. J. Reconstr. Microsurg. 38 (2022), 630-636.
7. Rodriguez, JR, T Yamamoto: A systematic stepwise method to perform a supermicrosurgical lymphovenous anastomosis. Ann. Plast. Surg. 88 (2021), 524-532.
8. Seward, C, M Skolny, C Brunelle, et al: A comprehensive review of bioimpedance spectroscopy as a diagnostic tool for the detection and measurement of breast cancer-related lymphedema. J. Surg. Oncol. 114 (2016), 537-542.
9. Qin, ES, MJ Bowen, WF Chen: Diagnostic accuracy of bioimpedance spectroscopy in patients with lymphedema: A retrospective cohort analysis. J. Plast. Reconstr Aes. 71 (2018), 1041-1050.
10. Hayashi, A, T Yamamoto, H Yoshimatsu, et al: Ultrasound visualization of the lymphatic vessels in the lower leg. Microsurg. 36 (2016), 397–401.
11. Monnin-Delhom, ED, BP Gallix, C Achard, et al: High resolution unenhanced computed tomography in patients with swollen legs. Lymphology. 35 (2002), 121-128.
12. Lee, DG, S Lee, KT Kim: Computed tomography-based quantitative analysis of fibrotic changes in skin and subcutaneous tissue in lower extremity lymphedema following gynecologic cancer surgery. Lymphat. Res. Biol. 20 (2022), 488-495.
13. Cellina, M, D Gibelli, C Martinenghi, et al: Non-contrast magnetic resonance lymphography (NCMRL) in cancer-related secondary lymphedema: acquisition technique and imaging findings. Radiol. Med. 126 (2021), 1477-1486.
14. Kim, G, K Donohoe, MP Smith, et al: Use of non-contrast MR in diagnosing secondary lymphedema of the upper extremities. Clin. Imag. 80 (2021), 400-405.
15. Cellina, M, G Oliva, A Menozzi, et al: Non-contrast magnetic resonance lymphangiography: An emerging technique for the study of lymphedema. Clin. Imag. 53 (2019), 126-133.
16. Arrivé, L, S Derhy, B Dahan, et al: Primary lower limb lymphoedema: Classification with non-contrast MR lymphography. Eur. Radiol. 28 (2018), 291-300.
17. Dayan, JH, I Wiser, R Verma, et al: Regional patterns of fluid and fat accumulation in patients with lower extremity lymphedema using magnetic resonance angiography. Plast. Reconstr. Surg. 145 (2020), 555-563.
18. Mihara, M, H Hara, M Narushima, et al: Indocyanine green lymphography is superior to lymphoscintigraphy in imaging diagnosis of secondary lymphedema of the lower limbs. J. Vasc. Surg.-Venous L. 1 (2013), 194-201.
19. Yamamoto, T, N Yamamoto, H Sakai, et al: Lymphedema quality of life score (LeQOLiS): A simple method for evaluation of subjective symptoms in extremity lymphedema patients. Plast. Reconstr. Surg. 142 (2018), 1.
20. Yamamoto, T, N Matsuda, T Todokoro, et al: Lower extremity lymphedema index: A simple method for severity evaluation of lower extremity lymphedema. Ann. Plast. Surg. 67 (2011), 637-640.
21. Yamamoto, T, M Narushima, K Doi, et al: Characteristic indocyanine green lymphography findings in lower extremity lymphedema: The generation of a novel lymphedema severity staging system using dermal backflow patterns. Plast. Reconstr. Surg. 127 (2011), 1979–1986.
22. Gregl, A, U Fischer, D von Heyden, et al: Computed tomography and nuclear spin tomography in peripheral lymphedema. Rofo. 143 (1985), 219-226.
23. Kageyama, T: Evaluation of characteristic non-contrast magnetic resonance lymphangiography findings based on indocyanine green lymphography. Microsurg. 42 (2022), 298-299.
24. Kageyama, T: Characteristic non-contrast magnetic resonance lymphography findings of secondary lower extremity lymphedema. J. Plast. Reconstr. Aes. 75 (2022), 893-939.
25. Cellina, M, G Oliva, A Menozzi, et al: Non-contrast magnetic resonance lymphangiography: An emerging technique for the study of lymphedema. Clin. Imag. 53 (2019), 126-133.
26. Narushima, M, T Yamamoto, F Ogata, et al: Indocyanine green lymphography findings in limb lymphedema. J. Reconstr. Microsurg. 32 (2016), 72-79.
27. Aschen, S, JC Zampell, S Elhadad, et al: Regulation of adipogenesis by lymphatic fluid stasis: Part II. Expression of adipose differentiation genes. Plast. Reconstr. Surg. 129 (2012), 838-847.
28. Gentili, F, FG Mazzei, I Monteleone, et al: Comparison of indocyanine green fluorescence lymphangiography and magnetic resonance lymphangiography to investigate lymphedema of the extremities. Ann. Ital. Chir. 92 (2021), 452-459.

29. Kim, G, MP Smith, KJ Donohoe, et al: MRI staging of upper extremity secondary lymphedema: Correlation with clinical measurements. Eur. Radiol. 30 (2020), 4686-4694.
30. Dayan, JH, I Wiser, R Verma, et al: Regional patterns of fluid and fat accumulation in patients with lower extremity lymphedema using magnetic resonance angiography. Plast. Reconstr. Surg. 145 (2020), 555-563.
31. Yamamoto, T, M Narushima, H Yoshimatsu, et al: Indocyanine green velocity: Lymph transportation capacity deterioration with progression of lymphedema. Ann. Plas. Surg. 71 (2013), 591-594.

Takumi Yamamoto, MD, PhD
Department of Plastic and Reconstructive Surgery
National Center for Global Health and Medicine
1-21-1 Toyama, Shinjuku-ku, Tokyo, 162-8655
Japan
Tel.: +81 3 3202 7181
Fax: +81 3 3207 1038
E-mail: tyamamoto-tky@umin.ac.jp